Monthly Notices of the ROYAL ASTRONOMICAL SOCIETY
MNRAS **489,** L75–L79 (2019)
Advance Access publication 2019 August 21
doi:10.1093/mnrasl/slz129

Using negative-latency gravitational wave alerts to detect prompt radio bursts from binary neutron star mergers with the Murchison Widefield Array

Clancy W. James ,[1★] Gemma E. Anderson ,[1] Linqing Wen,[2] Joel Bosveld,[2] Qi Chu,[2] Manoj Kovalam,[2] Teresa J. Slaven-Blair[2] and Andrew Williams[1]

[1] *International Centre for Radio Astronomy Research, Curtin University, GPO Box U1987, Perth, WA 6845, Australia*
[2] *OzGrav-UWA, Department of Physics, The University of Western Australia, Crawley, WA 6009, Australia*

Accepted 2019 August 16. Received 2019 July 31; in original form 2019 June 19

ABSTRACT

We examine how fast radio burst (FRB)-like signals predicted to be generated during the merger of a binary neutron star (BNS) may be detected in low-frequency radio observations triggered by the aLIGO/Virgo gravitational-wave detectors. The rapidity, directional accuracy, and sensitivity of follow-up observations with the Murchison Widefield Array (MWA) are considered. We show that with current methodology, the rapidity criterion fails for triggered MWA observations above 136 MHz for BNS mergers within the aLIGO/Virgo horizon, for which little dispersive delay is expected. A calculation of the expected reduction in response time by triggering on ‘negative latency’ alerts from aLIGO/Virgo observations of gravitational waves generated by the BNS inspiral is presented. This allows for observations up to 300 MHz where the radio signal is expected to be stronger. To compensate for the poor positional accuracy expected from these alerts, we propose a new MWA observational mode that is capable of viewing one-quarter of the sky. We show the sensitivity of this mode is sufficient to detect an FRB-like burst from an event similar to GW 170817 if it occurred during the ongoing aLIGO/Virgo third science run (O3).

Key words: gravitational waves – methods: observational – stars: neutron – radio continuum: transients.

1 INTRODUCTION

The detection of the first binary neutron star (BNS) merger GW 170817 (Abbott et al. 2017b) – also detected as GRB 170817A (Abbott et al. 2017d; Goldstein et al. 2017) – triggered a wide range of follow-up observations across the electromagnetic and particle spectrum (Abbott et al. 2017c; Albert et al. 2017). However, the delay in issuing the alert prevented most instruments from observing any prompt transient event. The utility of a rapid trigger–response system for capturing electromagnetic signatures from gravitational wave (GW) events produced by compact mergers that include at least one neutron star (NS) has been long recognized, with predictions for associated prompt radio, optical, X-ray, and gamma-ray emission (Paczynski 1986; Hansen & Lyutikov 2001; Cannon et al. 2012; Centrella, Nissanke & Williams 2012; Chu et al. 2016; Rowlinson & Anderson 2019). Consequently, the third science run, O3, of the aLIGO/Virgo GW detector network is issuing alerts for high-significance ‘superevents’ within minutes of detection. At least one high-significance BNS merger candidate has been detected.[1] The detection of fast radio bursts (FRBs; Lorimer et al. 2007; Thornton et al. 2013), which are extragalactic radio transients of millisecond duration with an unexplained origin, also motivates the search for prompt radio emission associated with BNS mergers. While BNS cannot explain repeating FRBs, which might produce bursts at a rate $>10^4$ Gpc^{-3} yr^{-1} (Ravi 2019), it is quite possible that FRBs belong to more than one class (Caleb, Spitler & Stappers 2018). Indeed, the archetypal repeating FRB, FRB 121102 (Spitler et al. 2014), must be uncharacteristic of the population(s) as a whole (James 2019). While the FRB rate of 200–1000 sky^{-1} day^{-1} (Lawrence et al. 2017) is much higher than that of BNS mergers, FRBs belong to a cosmological population (Shannon et al. 2018) extending well beyond the current BNS merger detection horizon of aLIGO/Virgo. The BNS merger event rate of 1540^{+3200}_{-1220} Gpc^{-3} yr^{-1} (Abbott et al. 2017b) is compatible with the non-repeating FRB

★ E-mail: clancy.james@curtin.edu.au

[1] As of 2019 July 24 (S190425z). S190510g and S190426c are also possible mergers involving a NS; S190518bb and S190524q have subsequently been retracted. See https://gracedb.ligo.org/latest/

rate of ∼2700 $\mathrm{Gpc^{-3}\ yr^{-1}}$ (Lu & Piro 2019). We use the term 'FRB-like' to cover the general case where BNS are predicted to produce short-duration dispersed bursts that may or may not constitute a significant fraction of the observed FRB population. A BNS merger could produce FRB-like emission from magnetic field interactions just prior to the merger during the inspiral, the disruption of fields at the point of merger, or post-merger due to either the interaction of a relativistic jet with the interstellar medium (ISM), pulsar-like emission from a supramassive, rapidly rotating, highly magnetized NS remnant (often referred to as a magnetar), or (if unstable) the collapse of this magnetar into a black hole (e.g. Usov & Katz 2000; Hansen & Lyutikov 2001; Lyutikov 2013; Totani 2013; Zhang 2014; Wang et al. 2016; Rowlinson & Anderson 2019). Low-frequency ($\lesssim$300 MHz) radio telescopes are our best hope for detecting FRB-like signals from BNS. They have large fields of view (FOVs) that allow them to efficiently search for poorly localized transients (e.g. Obenberger et al. 2014; Howell et al. 2015; Abbott et al. 2016; Kaplan et al. 2016; Anderson et al. 2018; Callister et al. 2019). Furthermore, the dispersive delay due to a distant radio signal's propagation through ionized gas in the ISM and intergalactic medium (IGM) can be minutes at low frequencies, providing extra time to repoint at a newly detected event (e.g. Kaplan et al. 2015; Yancey et al. 2015). However, BNS mergers detected during the O3 run will originate from the nearby Universe, where the dispersive delays may not be large enough to compensate for delays in a trigger–response system. We therefore propose a specific observational mode of the Murchison Widefield Array (MWA) to probe for prompt FRB-like radio bursts emitted by BNS mergers, which requires using 'negative-latency triggering' (triggers from detections of GW generated by the BNS inspiral) from the aLIGO/Virgo detector network during its O3 run.

2 EXPECTED RADIO BURST DELAY

A key characteristic of FRBs is their dispersion sweep, being the frequency-dependent delay due to ionized gas in interstellar and intergalactic media. The delay, $t_{\rm FRB}$, is given by

$$t_{\rm FRB} = 415\ {\rm DM} \left(\frac{\nu}{100\,{\rm MHz}}\right)^{-2}\ ({\rm ms}), \qquad (1)$$

where DM is the dispersion measure (total line-of-sight electron content, pc $\mathrm{cm^{-3}}$), and ν the observing frequency. The BNS merger detection horizon during the O3 aLIGO/Virgo run is estimated to be 170 Mpc, within which the event rate will be $32^{+66}_{-25}\ \mathrm{yr^{-1}}$ (based on BNS merger rate estimates by Abbott et al. 2017b). At these distances, the contribution of the IGM to the DM (∼0.21 pc $\mathrm{cm^{-3}\ Mpc^{-1}}$; Inoue 2004) will be much smaller than that due to the ISM of the Milky Way (∼40 pc $\mathrm{cm^{-3}}$ at high Galactic latitudes; Cordes & Lazio 2002), or that expected from its halo (50–80 pc $\mathrm{cm^{-3}}$; Prochaska & Zheng 2019). The observation of FRBs with DMs of 110 pc $\mathrm{cm^{-3}}$ (FRB 180729.J1316+55; CHIME/FRB Collaboration et al. 2019) and 114 pc $\mathrm{cm^{-3}}$ (FRB 171020; Shannon et al. 2018) favours the lower limit of predictions for the halo contribution, and rule out large DM contributions from merger ejecta or the host galaxy for the majority of bursts. Neither of these presumably nearby FRBs occurred during one of the aLIGO/Virgo science runs. We therefore adopt the following DM model, applicable to the majority of FRBs originating within the current aLIGO/Virgo horizon at distance D:

$${\rm DM} = 90 + 0.21\,\frac{D}{\rm Mpc}\ {\rm pc\,cm^{-3}}. \qquad (2)$$

3 PROPOSED OBSERVATION METHOD

The MWA is a low-frequency (80–300 MHz) radio telescope located in Outback Western Australia (Tingay et al. 2013; Wayth et al. 2018). It has a rapid-response capability that enables it to be on-target and observing within 6–14 s of receiving an external trigger (Hancock et al. in preparation). It is capable of triggering observations with the voltage capture system (VCS; Tremblay et al. 2015), which has a time resolution of 100 μs. The VCS allows for much greater sensitivity to dispersed pulses (e.g. Meyers et al. 2018; Xue et al. 2019) than can be obtained by performing image plane dedispersion searches for prompt emission on second time-scales using data output by the standard MWA correlator (e.g. Tingay et al. 2015; Sokolowski et al. 2018). The MWA is composed of 256 tiles – of which 128 can be used simultaneously – of 16 dipoles each. Beamforming on each tile is performed prior to digitization, i.e. unlike Low-Frequency Array (LOFAR; van Haarlem et al. 2013), a posteriori beamforming with digitized data from individual dipoles is not possible. The MWA FOV is thus limited to that of an individual tile (i.e. its primary beam), being 610 $\mathrm{deg^2}$ at the peak sensitivity of 150 MHz (Sokolowski et al. 2017). The standard MWA response to GW triggers uses an algorithm to maximize the overlap between tile pointing directions and GW event localization files (Kaplan et al. 2016). However, it takes several seconds to download and analyse the sky maps, and the typical GW localization error regions are usually bigger than the MWA beam size. Furthermore, localizations for negative-latency triggers will be even less accurate, being always generated at threshold (Section 4). The chance of viewing an FRB can be maximized by disabling 15 of 16 MWA dipoles on each tile, recovering the full FOV of a single dipole (the entire visible sky). Since dipole sensitivity tapers towards the horizon, we characterize the FOV in this mode as π sr, i.e. above an elevation of 30°, viewing 1/4 of all BNS mergers. Compared with MWA VCS observations using all 16 dipoles per tile, the loss of sensitivity will be approximately 16-fold. However, BNS mergers detected by aLIGO/VIRGO will be significantly closer than the majority of observed FRBs, largely compensating for this loss of sensitivity. We propose to trigger MWA's VCS whenever an aLIGO/Virgo template search with at least one mass consistent with a NS exceeds a pre-set threshold. Observations lasting a single minute with the VCS using a single dipole per tile will be adequate to catch the majority of proposed FRB-like signals predicted to be produced during a merger. Highly dispersed FRBs from the centres of local galaxies/clusters, or those propagating through much of the Milky Way's disc, may have DMs over ∼1000 pc $\mathrm{cm^{-3}}$ (Prochaska & Zheng 2019). These will be observable using the methods of Kaplan et al. (2016), which will also be sensitive to bursts emitted by any post-merger remnant.

4 NEGATIVE-LATENCY TRIGGERING

The time between the aLIGO/Virgo detection of a superevent during the O3 run and the submission time of alerts is currently 18–28 s.[2] Let us suppose we use MWA to trigger on the first BNS merger detected by any GW pipeline, rather than waiting for the most significant trigger over all pipelines, and that this alert is broadcast at the best alert time of 18 s. Adding the typical MWA trigger response time of $t_{\rm MWA} = 10$ s, we estimate a total delay between merger and observation of $t_{\rm obs} = 28$ s. Using equations (1) and (2),

[2]https://gracedb.ligo.org/latest/

an observational delay of $t_{obs} = 28$ s matches the dispersive delay of a 136 MHz signal generated at 170 Mpc (DM = 125.7 pc cm^{-3}), i.e. the maximum possible observing frequency that will allow us to observe an FRB-like signal associated with a BNS merger is $\nu_{max} = 136$ MHz. At the 40 Mpc distance of GW 170817 (Abbott et al. 2017a; Abbott et al. 2019), ν_{max} is even lower, at 121 MHz (DM = 98.4 pc cm^{-3}). Despite evidence from GHz observations that FRB emission is stronger with decreasing frequency (Macquart et al. 2019), MWA observations at 170–200 MHz did not detect seven FRBs discovered by the Australian Square Kilometre Array Pathfinder (ASKAP; Johnston et al. 2008) during simultaneous observations (Sokolowski et al. 2018). As discussed by Sokolowski et al. (2018), this suggests a low-frequency downturn in the spectral strength, possibly due to free–free absorption (Rybicki & Lightman 1986), e.g. in merger ejecta. Scattering due to inhomogeneities in the ISM (Bhat et al. 2004) and/or the IGM (Macquart & Koay 2013) would also spread the signal in time and reduce sensitivity, although this alone cannot explain the non-detection. Given FRBs have been observed at 400 MHz by CHIME/FRB Collaboration et al. (2019), a complete lack of ∼100 MHz emission seems unlikely. Furthermore, bursts emanating from within the aLIGO/Virgo horizon will be at least an order of magnitude closer, and therefore brighter, than those observed by ASKAP (Shannon et al. 2018). In order to catch these events at higher MWA frequencies (136–300 MHz), where any signal is likely to be stronger, we require negative-latency triggering.

4.1 Simulations using GW 170817

The principle of negative-latency triggering is simple: search for GWs produced by the inspiral of compact objects prior to their merger, and broadcast the alert as soon as the significance of a template waveform passes a pre-defined threshold, rather than waiting for the merger and the maximum sensitivity of a template to be reached (Cannon et al. 2012; Luan et al. 2012). It is specifically planned to be implemented in GW search algorithms, such as the Summed Parallel Infinite Impulse Response (SPIIR) pipeline (Hooper et al. 2012; Liu et al. 2012; Luan et al. 2012; Hooper 2013; Chu 2017; Guo et al. 2018). We analyse the trade-off in sensitivity and time using publicly available 2048 Hz clean GW data on GW 170817 from the LIGO Hanford ('H') and Livingston ('L') detectors (the Virgo signal-to-noise ratio, SNR, is negligible here compared to the SNRs of the two LIGO detectors; Vallisneri et al. 2015).[3] A time-domain template waveform is generated in PyCBC (Allen 2005; Allen et al. 2012; Dal Canton et al. 2014; Nitz et al. 2017, 2019) using the SpinTaylorT4 approximant, with a parameter set within the range of the best-fitting parameters found by Abbott et al. (2017b, 2018). The background power spectral density is estimated from the data prior to merger. A low-frequency cut-off of 20 Hz was applied. Negative-latency triggering is simulated by setting the predicted waveform shape to zero from a time t_{-ve} prior to the merger onwards. The network signal-to-noise ratio at t_{-ve}, SNR(t_{-ve}), is calculated from the individual SNRs on each detector as

$$\mathrm{SNR}(t_{-ve}) = \sqrt{\mathrm{SNR}_{\mathrm{L}}^2(t_{-ve}) + \mathrm{SNR}_{\mathrm{H}}^2(t_{-ve})}. \quad (3)$$

This is shown in Fig. 1, normalized by the peak value of 32.6 found for the SNR of GW 170817 at $t_{-ve} = 0$. This peak SNR is in close agreement with that found by aLIGO/VIRGO (Abbott et al. 2017b).

[3] https://www.gw-openscience.org/events/GW170817/

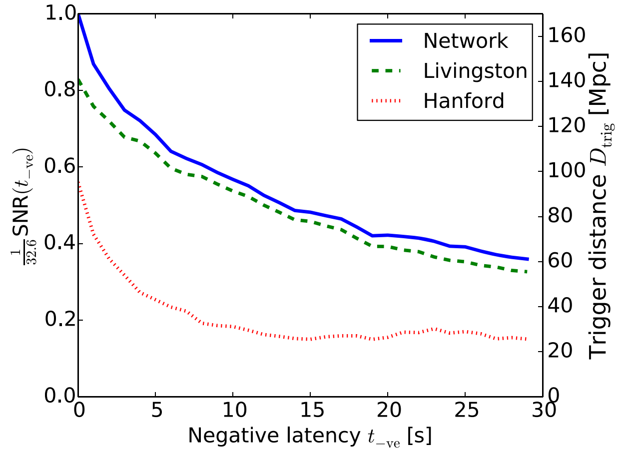

Figure 1. Signal-to-noise ratios (SNR; left-hand axis) of a negative-latency trigger applied to GW 170817 as a function of time (t_{-ve}) prior to the merger. Shown are the SNRs from the Livingston and Hanford detectors, and the network SNR from equation (3). It has been normalized by the peak network SNR value of 32.6 (at $t_{-ve} = 0$) to highlight the loss of sensitivity with increasing negative latency. The network SNR also gives the corresponding distance (D_{trig}; right-hand axis) at which a GW 170817-like event would equal the detection threshold at a time t_{-ve} in the aLIGO/Virgo O3 run.

Over the range $t_{-ve} \in$ 0–30 s, the SNR drops to one-third of its peak value.

Nearby BNS mergers will produce a stronger GW signal, resulting in the SNR passing the trigger threshold at earlier times. Conversely, events that produce a negative-latency trigger at an earlier t_{-ve} will have to be closer. We therefore define the trigger distance, $D_{trig}(t_{-ve})$, to be the distance at which a GW 170817-like event would cause a trigger at time t_{-ve}. Since the SNR of a GW event scales inversely with distance, $D_{trig}(t_{-ve})$ will be directly proportional to SNR(t_{-ve}). The constant of proportionality is set by the maximum BNS detection distance for the O3 run of $D_{max} = 170$ Mpc at $t_{-ve} = 0$. D_{trig} is shown in Fig. 1, using the same curves as SNR(t_{-ve}) via the right-hand y-axis.

The distance of an event is associated with a DM via equation (2). Applying this to D_{trig}, itself a function of t_{-ve}, produces DM(t_{-ve}), shown in Fig. 2. That is, a BNS merger passing the detection threshold at earlier times must be closer, and hence will have passed through less intervening material (and vice versa).

For a given frequency ν, the time delay $t_{FRB}(\mathrm{DM}, \nu)$ in the arrival of an FRB-like signal due to dispersion can be found through equation (1). In order to observe the event, the total response time (t_{obs}), less the time gained in negative latency (t_{-ve}), must be less than the dispersed arrival time of the FRB ($t_{DM}(\nu)$). Equivalently, there is a maximum observable frequency (ν_{max}) for which the above statement holds true, i.e.

$$t_{FRB}(\mathrm{DM}, \nu_{max}) = t_{obs} - t_{-ve}. \quad (4)$$

Solving equation (4) using the values of DM(t_{-ve}) given in Fig. 2 sets ν_{max} to the maximum possible observing frequency for which the MWA can be on target to observe an FRB-like signal associated with a merger as a function of negative latency. While nearby BNS mergers incur less dispersive delay, this is more than compensated for by the time gained through negative-latency triggering. Thus ν_{max} increases from 136 MHz at $t_{-ve} = 0$ to infinity when $t_{-ve} = t_{obs}$, where the dispersion delay ($t_{FRB}(\mathrm{DM}, \nu_{max})$) is no longer required to enable a follow-up observation. For the MWA, this maximum frequency is capped at 300 MHz.

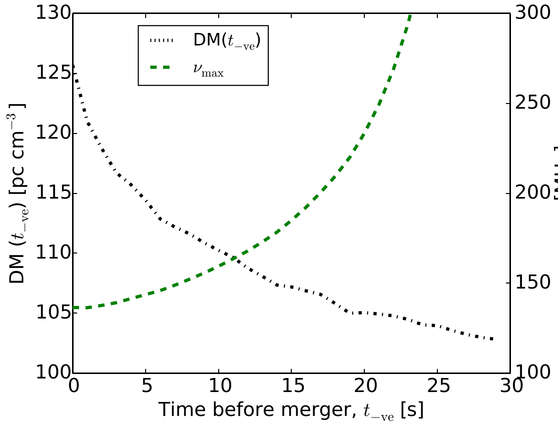

Figure 2. Expected dispersion measure (DM) for FRB-like events associated with BNS mergers as a function of t_{-ve} (left-hand axis, black dotted line). For an assumed total observational delay $t_{obs} = 28$ s, the corresponding peak frequency (ν_{max}) at which an FRB-like signal would be observable within the GW-MWA response time of 28 s (right-hand axis, green dot–dashed line).

Fig. 2 suggests that triggered observations should use a tuneable frequency band based on the negative latency of the trigger. As the exact relation between t_{-ve} and ν_{max} will depend on the shape of the GW signal, we suggest using a split frequency band (e.g. 112–127 MHz and 216–231 MHz). This provides a good compromise between greater detection sensitivity at high frequencies to nearby events, and a greater dispersive delay at low frequencies allowing more numerous distant events to be observed.

Given the lack of definitive predictions for the radio strength of FRB-like signals from BNS mergers, it is currently impossible to translate the gains from negative-latency triggering into a hard prediction for the detection rate of FRB-like signals from BNS mergers. Rather, our prescription is to use a negative-latency trigger, allowing observations at the highest possible frequency, to maximize the chance of observing any such burst.

We can demonstrate that our MWA observational mode proposed in Section 3 is sufficiently sensitive to detect FRB-like emission from BNS mergers in at least one plausible scenario. Assuming that BNS mergers are responsible for a significant fraction of the detected non-repeating FRB population, it becomes possible to use the (poor) constraints on this population to make event-rate predictions. For example, in Supplemental Material, we present a calculation based on the properties of the observed FRB population (Shannon et al. 2018; Lu & Piro 2019; Macquart et al. 2019). For the distance estimated by Mahony et al. (2018), FRB 171020 places the strongest constraints on FRB emission in the MWA band (Sokolowski et al. 2018). Using this to set an absolute scale for emission strength at MWA frequencies, our conclusion *for this particular calculation* is that all FRB-like bursts produced by BNS mergers within 30 Mpc will be detectable with the MWA if they are located within the π sr observable sky with this mode. At larger distances, there is a decreasing probability that FRB-like signals will be sufficiently bright to be detectable. For example, GW 170817 occurred at a distance of 40 Mpc, corresponding to an estimated 80 per cent probability of producing a detectable FRB-like signal. If a similar event were to occur during the aLIGO/Virgo O3 run, our proposed observational mode would either detect an FRB-like burst, or place strong constraints on BNS mergers as FRB progenitors.

5 CONCLUSION

The detection of prompt FRB-like signals associated with BNS mergers requires a radio instrument of sufficient sensitivity capable of being on-target before the arrival of a burst. We have described a unique observational strategy whereby candidate BNS GW events are identified with negative latency (i.e. prior to merger) by aLIGO/Virgo, and trigger automatic and rapid MWA follow-up observations. This gain in response time would allow us to trigger higher frequency observations (up to 300 MHz) with the MWA, where any burst signal is less likely to suffer from scatter broadening or free–free absorption.

Other low-frequency radio telescopes, such as the LOFAR (van Haarlem et al. 2013) and the Long Wavelength Array (LWA; Ellingson et al. 2009), may also be able to take advantage of negative-latency triggers broadcast by aLIGO/Virgo, improving global sky coverage.

For a plausible model of FRB-like emission from BNS mergers (see Supplementary Material), we have shown that this observational method is sufficiently sensitive to allow for a detection. This proposed experiment presents the best, and perhaps only, chance of testing whether FRB-like signals are produced during a BNS merger, *and is feasible during the O3 run of aLIGO/Virgo*.

ACKNOWLEDGEMENTS

GEA is the recipient of an Australian Research Council Discovery Early Career Researcher Award (project number DE180100346). This work was supported in part by the Australian Research Council Centre of Excellence for Gravitational Wave Discovery (OzGrav; project number CE170100004). This research has made use of data, software, and/or web tools obtained from the Gravitational Wave Open Science Center (https://www.gw-openscience.org), a service of LIGO Laboratory, the LIGO Scientific Collaboration, and the Virgo Collaboration. LIGO is funded by the US National Science Foundation. Virgo is funded by the French Centre National de Recherche Scientifique (CNRS), the Italian Istituto Nazionale della Fisica Nucleare (INFN), and the Dutch Nikhef, with contributions by Polish and Hungarian institutes. Calculations in this work use NumPy (Oliphant 2006) and MATPLOTLIB libraries (Hunter 2007).

REFERENCES

Abbott B. P. et al., 2016, ApJ, 826, L13
Abbott B. P. et al., 2017a, Phys. Rev. Lett., 119, 141101
Abbott B. P. et al., 2017b, Phys. Rev. Lett., 119, 161101
Abbott B. P. et al., 2017c, ApJ, 848, L12
Abbott B. P. et al., 2017d, ApJ, 848, L13
Abbott B. P. et al., 2018, Phys. Rev. Lett., 121, 161101
Abbott B. P. et al., 2019, Phys. Rev. X, 9, 011001
Albert A. et al., 2017, ApJ, 850, L35
Allen B., 2005, Phys. Rev. D, 71, 062001
Allen B., Anderson W. G., Brady P. R., Brown D. A., Creighton J. D. E., 2012, Phys. Rev. D, 85, 122006
Anderson M. M. et al., 2018, ApJ, 864, 22
Bhat N. D. R., Cordes J. M., Camilo F., Nice D. J., Lorimer D. R., 2004, ApJ, 605, 759
Caleb M., Spitler L. G., Stappers B. W., 2018, Nat. Astron., 2, 839
Callister T. A. et al., 2019, ApJ, 877, L39
Cannon K. et al., 2012, ApJ, 748, 136
Centrella J., Nissanke S., Williams R., 2012, in Griffin E., Hanisch R., Seaman R., eds, Proc. IAU Symp. Vol. 285, New Horizons in Time-Domain Astronomy. Cambridge Univ. Press, Cambridge, p. 191
CHIME/FRB Collaboration et al., 2019, Nature, 566, 230

Chu Q., 2017, PhD thesis, The University of Western Australia
Chu Q., Howell E. J., Rowlinson A., Gao H., Zhang B., Tingay S. J., Boër M., Wen L., 2016, MNRAS, 459, 121
Cordes J. M., Lazio T. J. W., 2002, preprint (arXiv:astro-ph/0207156)
Dal Canton T. et al., 2014, Phys. Rev. D, 90, 082004
Ellingson S. W., Clarke T. E., Cohen A., Craig J., Kassim N. E., Pihlstrom Y., Rickard L. J., Taylor G. B., 2009, Proc. IEEE, 97, 1421
Goldstein A. et al., 2017, ApJ, 848, L14
Guo X., Chu Q., Chung S. K., Du Z., Wen L., Gu Y., 2018, Comput. Phys. Commun., 231, 62
Hansen B. M. S., Lyutikov M., 2001, MNRAS, 322, 695
Hooper S., 2013, PhD thesis, The University of Western Australia
Hooper S., Chung S. K., Luan J., Blair D., Chen Y., Wen L., 2012, Phys. Rev. D, 86, 024012
Howell E. J. et al., 2015, Publ. Astron. Soc. Aust., 32, e046
Hunter J. D., 2007, Comput. Sci. Eng., 9, 90
Inoue S., 2004, MNRAS, 348, 999
James C. W., 2019, MNRAS, 486, 5934
Johnston S. et al., 2008, Exp. Astron., 22, 151
Kaplan D. L. et al., 2015, ApJ, 814, L25
Kaplan D. L., Murphy T., Rowlinson A., Croft S. D., Wayth R. B., Trott C. M., 2016, Publ. Astron. Soc. Aust., 33, e050
Lawrence E., Vander Wiel S., Law C., Burke Spolaor S., Bower G. C., 2017, AJ, 154, 117
Liu Y., Du Z., Chung S., Hooper S., Blair D., Wen L., 2012, Classical Quantum Gravity, 29, 15
Lorimer D. R., Bailes M., McLaughlin M. A., Narkevic D. J., Crawford F., 2007, Science, 318, 777
Lu W., Piro A. L., 2019, preprint (arXiv:1903.00014)
Luan J., Hooper S., Wen L., Chen Y., 2012, Phys. Rev. D, 85, 102002
Lyutikov M., 2013, ApJ, 768, 63
Macquart J.-P., Koay J. Y., 2013, ApJ, 776, 125
Macquart J.-P., Shannon R. M., Bannister K. W., James C. W., Ekers R. D., Bunton J. D., 2019, ApJ, 872, L19
Mahony E. K. et al., 2018, ApJ, 867, L10
Meyers B. W. et al., 2018, ApJ, 869, 134
Nitz A. H., Dent T., Dal Canton T., Fairhurst S., Brown D. A., 2017, ApJ, 849, 118
Nitz A. et al., 2019, gwastro/pycbc: PyCBC Release v1.13.6
Obenberger K. S. et al., 2014, ApJ, 785, 27
Oliphant T., 2006, Guide to NumPy. Trelgol Publishing, USA
Paczynski B., 1986, ApJ, 308, L43
Prochaska J. X., Zheng Y., 2019, MNRAS, 485, 648
Ravi V., 2019, Nat. Astron.
Rowlinson A., Anderson G. E., 2019, MNRAS, doi: 10.1093/mnras/stz2295
Rybicki G. B., Lightman A. P., 1986, Radiative Processes in Astrophysics. Wiley, New York
Shannon R. M. et al., 2018, Nature, 562, 386
Sokolowski M. et al., 2017, Publ. Astron. Soc. Aust., 34, e062
Sokolowski M. et al., 2018, ApJ, 867, L12
Spitler L. G. et al., 2014, ApJ, 790, 101
Thornton D. et al., 2013, Science, 341, 53
Tingay S. J. et al., 2013, Publ. Astron. Soc. Aust., 30, e007
Tingay S. J. et al., 2015, AJ, 150, 199
Totani T., 2013, PASJ, 65, L12
Tremblay S. E. et al., 2015, Publ. Astron. Soc. Aust., 32, e005
Usov V. V., Katz J. I., 2000, A&A, 364, 655
Vallisneri M., Kanner J., Williams R., Weinstein A., Stephens B., 2015, J. Phys. Conf. Ser., 610, 012021
van Haarlem M. P. et al., 2013, A&A, 556, A2
Wang J.-S., Yang Y.-P., Wu X.-F., Dai Z.-G., Wang F.-Y., 2016, ApJ, 822, L7
Wayth R. B. et al., 2018, Publ. Astron. Soc. Aust., 35, e033
Xue M., Ord S. M., Tremblay S. E., Bhat N. D. R., Sobey C., Meyers B. W., McSweeney S. J., Swainston N. A., 2019, Publ. Astron. Soc. Aust., 36, e025
Yancey C. C. et al., 2015, ApJ, 812, 168
Zhang B., 2014, ApJ, 780, L21

SUPPORTING INFORMATION

Supplementary data are available at *MNRASL* online.

Please note: Oxford University Press is not responsible for the content or functionality of any supporting materials supplied by the authors. Any queries (other than missing material) should be directed to the corresponding author for the article.

This paper has been typeset from a TEX/LATEX file prepared by the author.